

1 **Translating *in vivo* metabolomic analysis of succinate dehydrogenase deficient tumours**  
2 **into clinical utility**

3

4 **Ruth T Casey<sup>1,2</sup>, Mary A McLean<sup>3</sup>, Basetti Madhu<sup>3</sup>, Benjamin. G Challis<sup>2</sup>, Rogier. ten**  
5 **Hoopen<sup>4</sup>, Thomas. Roberts<sup>5</sup>, Graeme. R. Clark<sup>1</sup>, Deborah Pittfield<sup>2</sup>, Helen L Simpson<sup>6</sup>,**  
6 **Venkata R Bulusu<sup>7</sup>, Kieren Allinson<sup>8</sup>, Lisa Happerfield<sup>9</sup>, Soo-Mi Park<sup>1</sup>, Alison Marker<sup>8</sup>,**  
7 **Olivier Giger<sup>4</sup>, Eamonn R Maher <sup>\*1</sup>, Ferdia A Gallagher <sup>\*3, 10</sup>.**

8 1. Department of Medical Genetics, University of Cambridge and NIHR Cambridge  
9 Biomedical Research Centre and Cancer Research UK Cambridge Centre, CB2 0QQ, United  
10 Kingdom.

11 2. Department of Endocrinology, Cambridge University NHS Foundation Trust, Cambridge,  
12 CB2 0QQ, United Kingdom.

13 3. Cancer Research UK Cambridge Institute, University of Cambridge, Li Ka Shing Centre,  
14 Robinson Way, Cambridge CB2 0RE, UK

15 4. Department of Pathology, University of Cambridge, Addenbrooke's Hospital, Cambridge,  
16 CB2 0QQ, UK.

17 5. Haematology Oncology Diagnostic Service (HODS), Cambridge University NHS  
18 Foundation Trust, Cambridge, CB2 0QQ, United Kingdom.

19 6. Department of Diabetes and Endocrinology, University College London Hospitals, NHS  
20 Foundation Trust, London, NW1 2PG UK

21 7. Department of Medical Oncology, Cambridge University NHS Foundation Trust,  
22 Cambridge, CB2 0QQ, United Kingdom.

23 8. Department of Histopathology Cambridge University NHS Foundation Trust and Cancer  
24 Research UK Cambridge Centre Cambridge, CB2 0QQ, United Kingdom.

25 9. Department of Immunohistochemistry, Cambridge University NHS Foundation Trust,  
26 Cambridge, CB2 0QQ, United Kingdom.

27 10. Department of Radiology, Cambridge University NHS Foundation Trust, CB2 0QQ,  
28 United Kingdom.

29 **\*= joint last author**

30 **Corresponding author: Dr Ruth Casey, Department of Medical Genetics, University of**  
31 **Cambridge and NIHR Cambridge Biomedical Research Centre and Cancer Research**  
32 **UK Cambridge Centre, CB2 0QQ, United Kingdom.**

33 **Mobile: 07401 179473, Email: rc674@medschl.cam.ac.uk**

34 **Running title: *In vivo* metabolomic analysis of succinate dehydrogenase deficient**  
35 **tumours**

36 **Key words: Translational, metabolic cancer, metabolomics, hereditary, imaging**  
37 **technique**

38

39 **Word count: 3000**

40 **References: 30**

41 **Figures: 5**

42 **Tables 1**

43 **Supplementary figures: 1**

44 **Supplementary tables: 2**

45 **The authors have nothing to declare and there are no conflict of interests to report.**

46

47 **Disclosure: The authors have declared no conflicts of interest.**

48

49 **To date this research was presented as an abstract at the European Congress of**  
50 **Endocrinology in Lisbon in May 2017.**

51

52

53

54

55

56

57

58

59

60

61

62

63

64 **Abstract**

65 *Purpose:* Mutations in the mitochondrial enzyme succinate dehydrogenase (SDH) subunit  
66 genes are associated with a wide spectrum of tumours including pheochromocytoma and  
67 paraganglioma (PPGL) <sup>1,2</sup>, gastrointestinal stromal tumours (GIST) <sup>3</sup>, renal cell carcinoma  
68 (RCC) <sup>4</sup> and pituitary adenomas<sup>5</sup>. SDH-related tumorigenesis is believed to be secondary to  
69 accumulation of the oncometabolite succinate. Our aim was to investigate the potential  
70 clinical applications of MRI spectroscopy (<sup>1</sup>H-MRS) in a range of suspected SDH-related  
71 tumours.

72 *Patients and methods:* Fifteen patients were recruited to this study. Respiratory-gated single-  
73 voxel <sup>1</sup>H-MRS was performed at 3T to quantify the content of succinate at 2.4 ppm and  
74 choline at 3.22 ppm.

75 *Results:* A succinate peak was seen in six patients, all of whom had a germline *SDHx*  
76 mutation or loss of SDHB by immunohistochemistry. A succinate peak was also detected in  
77 two patients with a metastatic wild-type GIST (wtGIST) and no detectable germline *SDHx*  
78 mutation but a somatic epimutation in *SDHC*. Three patients without a tumour succinate peak  
79 retained SDHB expression, consistent with SDH functionality. In six cases with a borderline  
80 or absent peak, technical difficulties such as motion artefact rendered <sup>1</sup>H-MRS difficult to  
81 interpret. Sequential imaging in a patient with a metastatic abdominal paraganglioma  
82 demonstrated loss of the succinate peak after four cycles of [<sup>177</sup>Lu]-DOTATATE, with a  
83 corresponding biochemical response in normetanephrine.

84 *Conclusions:* This study has demonstrated the translation into clinical practice of *in vivo*  
85 metabolomic analysis using <sup>1</sup>H-MRS in patients with SDH-deficient tumours. Potential  
86 applications include non-invasive diagnosis and disease stratification, as well as monitoring  
87 of tumour response to targeted treatments.

## 88 Introduction

89 The succinate dehydrogenase (SDH) enzyme is composed of four subunits (A-D) and has a  
90 key role in the Krebs cycle and oxidative phosphorylation<sup>6</sup>. In the past two decades germline  
91 mutations in the genes encoding the four SDH subunits (*SDHA/SDHB/SDHC/SDHD*),  
92 collectively known as *SDHx* have emerged as an important cause of human neoplasia and a  
93 paradigm for the role of disordered cellular metabolism in oncogenesis<sup>1-5,7</sup>. *SDHx* mutations  
94 were described initially in association with head and neck paragangliomas (derived from  
95 parasympathetic ganglia) and in pheochromocytomas and paragangliomas (PPGL, derived  
96 from sympathetic ganglia and often secreting catecholamines)<sup>1,2</sup>. It is now recognised that  
97 approximately 40% of PPGL patients harbour a germline mutation in an inherited PPGL gene  
98 and *SDHx* mutations are the most common cause of PPGL predisposition<sup>9</sup>. In addition,  
99 germline *SDHB* mutations are associated with a high risk of malignancy in PPGL<sup>9</sup>. Other  
100 tumour types associated with *SDHx* mutations include gastrointestinal stromal tumours  
101 (GISTs) and renal cell carcinomas (RCCs)<sup>10-13</sup>. GISTs are mesenchymal tumours of the  
102 gastrointestinal tract and in adults usually associated with somatic activating mutations in the  
103 *KIT* or *PDGFRA* genes<sup>3,11</sup>. However GISTs without *KIT* and *PDGFRA* gene mutations<sup>3</sup>,  
104 known as wild-type (wtGIST), account for 15% of adult and 85% of paediatric GIST tumours  
105 and recent studies suggest that up to 88% of wtGIST are SDH-deficient<sup>11</sup>. wtGIST with  
106 SDH-deficiency may harbour a germline *SDHx* mutation (75% of cases) or an *SDHC* gene  
107 epimutation with hypermethylation of the promoter region<sup>11</sup>. Only about a third of patients  
108 with SDH-deficient wtGIST achieve disease stabilisation with imatinib therapy<sup>12</sup> and the risk  
109 of metastatic disease is higher for SDH-deficient GIST compared to conventional GIST<sup>11,12</sup>.  
110 *SDHx*-associated RCC may present in patients with a personal or family history of PPGL or  
111 may present with an RCC-only phenotype<sup>13</sup>. Finally germline *SDHx* mutations have been  
112 described in rare patients with pituitary adenomas<sup>10</sup>. Despite recent advances in the

113 understanding of the *SDHx* genes, there are many areas of unmet clinical need including a  
114 lack of robust biomarkers to predict aggressive biological behaviour and to inform on clinical  
115 surveillance and management<sup>14</sup>.  
116 Succinate has been shown to be elevated by 100-fold in *SDHx*-mutated PPGL tumours *ex-*  
117 *vivo* compared with non-*SDHx* mutated PPGL tumours<sup>15</sup>. Recently, *in vivo* detection of  
118 succinate by MR spectroscopy was reported in two patient cohorts with SDH deficient  
119 PPGL<sup>16, 17</sup>. Similarly, the non-invasive detection of 2-hydroxyglutarate with <sup>1</sup>H-MRS has  
120 been demonstrated in glioma in patients with a gain of function mutation in another citric  
121 acid cycle enzyme, isocitrate dehydrogenase 1 (IDH1)<sup>18</sup>. The ability to measure succinate *in*  
122 *vivo* has a number of important potential clinical applications including early identification of  
123 SDH deficiency, which can enable tailored patient surveillance and management. *In vivo*  
124 detection of succinate accumulation could also serve to verify genetic variant pathogenicity in  
125 the era of next generation sequencing. The aim of this study was to investigate the role of <sup>1</sup>H-  
126 MRS in detecting abnormally elevated succinate *in vivo* in patients with suspected SDH  
127 deficient tumours, expanding the applications of <sup>1</sup>H-MRS in SDH deficient tumorigenesis to  
128 include GIST and pituitary adenoma for the first time and to explore the technique as a  
129 potential non-invasive biomarker of treatment response.

130

## 131 **Methods**

### 132 Patient selection

133 This study was performed as a prospective case series and subjects were recruited from a  
134 dedicated neuroendocrine tumour clinic and a national paediatric and adult wild-type  
135 (PAWS) GIST clinic in Cambridge University NHS Foundation Trust. Suitable patients were  
136 identified based on *SDHx* germline status, suspicious clinical phenotype (metastatic PPGL,

137 paraganglioma or wtGIST) and/or immunohistochemistry of tumour tissue showing absent  
138 SDHB immunostaining. A minimum tumour size threshold of 1.5cm was applied for  
139 inclusion into the study. All participants gave written informed consent and the study was  
140 approved by Cambridge South Research Ethics Committee.

141

#### 142 MRS Analysis

143 Both SAGE (GE Healthcare, Waukesha, WI) and LCModel<sup>19</sup> spectroscopy analysis  
144 programmes were used to reconstruct, analyze and display spectra. For each metabolite,  
145 LCModel reports both peak area and the estimated uncertainty in fitting of the peak (%SD).  
146 This uncertainty measure was used to stratify the results using the following algorithm: 1) if  
147 %SD of choline was >15%, the spectrum was discarded as a technical failure, because it was  
148 assumed that choline should be detectable in a metabolically active tumour, such that  
149 SD>15% would indicate probable data quality issues; 2) succinate detection was taken as  
150 positive if its %SD was <50%, and negative if it was >50%. The succinate to choline ratio  
151 was quantified (SCR), the full width at half maximum height (FWHM) of the water peak in  
152 Hz was measured in SAGE and recorded as an additional data quality metric, and an expert  
153 spectroscopist was asked to rate whether detected succinate peaks were convincing or  
154 unconvincing based on data displayed both in LCModel and in SAGE.

155

#### 156 Statistical methods, <sup>1</sup>H-MRS data acquisition, Germline genetic analysis, SDHB

#### 157 Immunohistochemistry, SDHC hypermethylation analysis and measurement of succinate in ex 158 vivo tissue samples

159 See supplementary data.

160

161 **Results**

162 Patients and clinical phenotype

163 Fifteen subjects (6 females, 9 males; mean age 40 years (range 21-80 years) were studied.  
164 Seven wtGIST, three unilateral adrenal pheochromocytomas, three abdominal PGL's, a  
165 large left glomus PGL and a non-functioning pituitary macroadenoma were examined. Nine  
166 patients (60%) had metastatic disease: six with wtGIST, two with an abdominal  
167 paraganglioma and one with a unilateral pheochromocytoma. The liver was the most  
168 common site for metastases (7/9, 77.7%). Three patients had multicentric primary tumours,  
169 including subject #5 who presented with a metastatic wtGIST and was subsequently  
170 diagnosed with a 1.9 cm carotid body PGL (figure 2d, case 5), subject #9 with an abdominal  
171 paraganglioma and a small left sided 1.5 cm carotid paraganglioma (figure 3b, case 9), and  
172 subject #8 with a large left sided glomus paraganglioma and a 2 cm prolactin secreting  
173 pituitary adenoma (figure S1, case 8). Only two patients had a positive family history, (Table  
174 1: case 2 and case 6).

175 Genotype

176 A germline mutation in a *SDHx* gene was identified in 9/15 (60%) of subjects: 5 in *SDHB* (4  
177 missense variants and 1 truncating variant) and 4 in *SDHA* (1 missense and 3 truncating).  
178 Two further patients were diagnosed with a somatic *SDHC* epimutation (Table 1).

179

180 <sup>1</sup>H-MRS succinate analysis

181 The <sup>1</sup>H-MRS characteristics of the 15 patients are shown in Supplementary Table S1. The  
182 mean size of the tumour selected for spectra acquisition was 5.5 cm (median: 3.3 cm, range:  
183 1.8-12 cm). The liver was the most common site to be assessed (n = 6), but good quality



184 spectra were also obtained from the pituitary (n = 1), and PPGL tumours (n = 5). The subjects  
185 were divided into four groups according to whether a succinate tumour peak was: present,  
186 absent, a borderline peak was detected, or technical failure prevented interpretation of the  
187 spectra.

188

189 Succinate peak detected

190 Succinate was detected at 2.4 ppm in 6 patients (50 %). The mean SCR in these patients was  
191 1.3 (SD  $\pm$  0.71) and the mean tumour size in those six patients with reliable succinate peak  
192 detection was 4.8 cm (SD  $\pm$  2.94, range 2.3-9 cm). The *in vivo* detection of succinate on <sup>1</sup>H-  
193 MRS correlated with tumour SDH deficiency: 4 of the 6 cases had a germline *SDHx* mutation  
194 and loss of SDHB expression on immunohistochemistry and a somatic *SDHC* epimutation  
195 was detected in 2 of the 6 (Figure 1).

196

197

198 Borderline succinate peak detected

199 A borderline succinate peak was detected in two subjects. Patient #8 with a germline *SDHB*  
200 mutation (c.600G>T p.Trp200Cys) and a glomus paraganglioma, demonstrated an SCR of  
201 1.19; however the linewidth (29 Hz) was so broad due to the proximity of metallic dental  
202 work that the peak assignments were not reliable (Figure S1). Patient #7 with a metastatic  
203 pheochromocytoma and no detectable germline *SDHx* mutation demonstrated an SCR of  
204 0.18 but the LCModel detected a very small succinate peak at 2.4 ppm; this patient did not  
205 undergo surgery or a diagnostic biopsy and therefore no tissue was available for further  
206 analysis and therefore we have classified this case as borderline.

207 No succinate peak

208 No succinate peak was detected in three subjects. Patient #4 had a metastatic wtGIST with no  
209 detectable germline *SDHx* mutation and preserved SDHB protein expression in the tumour  
210 tissue; choline was confidently fitted on LCModel but no succinate was seen. Patient #6  
211 demonstrated a good quality spectrum from the remnant pituitary adenoma; choline was  
212 detected on LCModel and SAGE processing but no succinate was detected and this finding  
213 was consistent with the preservation of SDHB protein expression in the pituitary tumour by  
214 immunohistochemistry (Figure 4). Patient #10 had no detectable germline *SDHx* mutation  
215 and preserved SDHB protein expression in the tumour tissue; choline was detected in the  
216 tumour on <sup>1</sup>H-MRS but succinate was not detected.

217

218

219 Technical failure

220 Technical failure occurred in four patients (26%). Patient #12 demonstrated no reliable  
221 detection of succinate or choline due to motion artefact and a low signal-to-noise ratio (SNR),  
222 which was probably due to inconsistent breathing as the voxel was at the edge of the liver. A  
223 small rib metastasis was imaged in patient #13 but only a pure lipid spectrum was obtained  
224 from this challenging location. A metastasis on the edge of the liver was imaged in patient  
225 #14, where again inconsistent respiration probably led to displacement of the voxel into  
226 adjacent adipose tissue. Finally, patient #15 had a unilateral pheochromocytoma with a large  
227 volume of blood, whose paramagnetic properties may have affected acquisition leading to  
228 low SNR (Supplementary Table S1).

229

230 Sequential <sup>1</sup>H-MRS succinate analysis

231 Subject #2 with a metastatic paraganglioma to the lung, bone and lymph node and a germline  
232 *SDHB* mutation (c.268C>T p.Arg90\*) underwent <sup>1</sup>H-MRS on a large pelvic nodal metastasis  
233 prior to treatment with four cycles of lutetium 177-labelled peptide receptor radionuclide  
234 therapy. Succinate and choline peaks were detected with an SCR of 1.32 (Figures 5a, 5b).  
235 Following four cycles of treatment, a repeat <sup>1</sup>H-MRS examination on the same pelvic nodal  
236 metastases revealed a choline peak but no succinate peak (Figure 5c). Though the MRI  
237 imaging features of the metastatic lesions were unchanged pre- and post-treatment, the loss of  
238 a succinate peak was correlated with a reduction in plasma normetanephrine levels (from  
239 1861 to 1193 pmol/L) and tumour avidity on <sup>18</sup>F-fluorodeoxyglucose Positron Emission  
240 Tomography/Computed Tomography (FDG-PET/CT; standard uptake value of 16.1 pre-  
241 treatment and 9.3 post-treatment; Figure 5d-f). The detection of choline on the acquired  
242 spectra both before and after treatment indicates that tumour necrosis is unlikely to account  
243 for the absent succinate peak post treatment.

244 A sequential <sup>1</sup>H-MRS study was performed on patient #5 due to evidence of progressive  
245 disease on surveillance CT, despite treatment with a multi-kinase inhibitor, regorafenib.  
246 Serial <sup>1</sup>H-MRS demonstrated a larger succinate peak compared to the first study (Figure 2d  
247 and 2e) and this correlated with the FDG avidity on PET/CT pre-treatment and ten months  
248 post-treatment, which demonstrated an increase in disease burden and avidity (SUV: 15.1 and  
249 27.1 respectively, Figures 2f-g).

250 Repeatability of <sup>1</sup>H-MRS was evaluated in two patients by investigating different tumour  
251 deposits during the same study examination (case#5) and the same tumour deposit twice  
252 during the same study examination (case#1). The results for succinate: choline were almost  
253 identical in these two cases, suggesting good test reproducibility (Supplementary Table 2)

254

255 **Discussion**

256 This proof-of-principle study has demonstrated that detection of a succinate peak and an  
257 increased succinate to choline ratio were specific for a variety of SDH-deficient tumour  
258 types. All six tumours with a positive succinate peak and elevated SCR were associated with  
259 a germline *SDHx* mutation (n = 4) or an *SDHC* epimutation (n = 2). In addition, the three  
260 subjects with absent succinate peaks but adequate <sup>1</sup>H-MRS, demonstrated preservation of  
261 SDHB expression in the tumour analyzed. Our findings are complementary to a previous  
262 study in which <sup>1</sup>H-MRS was applied to 9 patients with paraganglioma and a succinate peak  
263 was detected in all 5 with an *SDHx* mutation but not in the 4 patients without a mutation<sup>16</sup>.  
264 We have demonstrated for the first time that <sup>1</sup>H-MRS can also be used to determine the SDH  
265 status of GISTs and pituitary adenomas and that a succinate peak can be detected in SDH-  
266 deficient tumours with epigenetic inactivation of *SDHC*. There are a wide variety of  
267 situations in which <sup>1</sup>H-MRS might have clinical utility. Potential diagnostic applications of  
268 this new approach include: (a) assessing the pathogenicity of patients with a germline SDHx  
269 variants of uncertain significance and a potentially SDH-related tumour; (b) investigating  
270 possible metastatic lesions e.g. in the liver, in patients with a germline *SDHx* mutation and a  
271 primary SDH-deficient tumour; (c) assessing patients with multiple primary tumours to  
272 determine if all are SDH-deficient; (d) identifying patients without a detectable germline  
273 *SDHx* mutation who might benefit from specialist genetic investigations such as *SDHC*  
274 promoter methylation status; and (e) assessing SDH tumour status pre-operatively  
275 particularly for patients with possible wtGIST as standard adjuvant treatment with imatinib  
276 has proven to be less effective in patients with SDH-deficient disease<sup>12</sup>.  
277 Notably, here we have used the presence of a choline signal as an internal control for viable  
278 tissue to discriminate technical failures from a negative finding. To avoid issues of partial  
279 voluming effects within smaller tumours, the voxel for MRS analysis was chosen to fully

280 include tumour where possible. We did not detect a statistically significant correlation  
281 between tumour size and succinate/choline ratio although there was a trend towards  
282 significance. This trend is the opposite of what would be expected if necrosis was artificially  
283 lowering the overall succinate levels in large tumours, and therefore suggests that the method  
284 is measuring real differences in succinate, which are independent of tumour size. However,  
285 we recommend using a size threshold of greater than 2 cm where possible to improve the  
286 sensitivity of the test.

287 There is increasing interest in understanding the metabolic adaptations that occur during  
288 tumorigenesis and how these might be exploited for novel therapeutic interventions.  
289 Increased production of lactate during aerobic glycolysis in most cancers, or the Warburg  
290 effect, is the best known example of this. SDH-related cancers provides a paradigm for  
291 investigating tumour metabolism as succinate is thought to act as an oncometabolite and to  
292 drive tumorigenesis<sup>6</sup>. Succinate inhibits 2-oxoglutarate-dependent dioxygenases including  
293 DNA and histone demethylases and hypoxic gene response regulators. As a consequence,  
294 SDH-deficient tumours demonstrate epigenetic abnormalities, an activated hypoxic gene  
295 response and more recently there is evidence that succinate may have a paracrine effect on  
296 stromal tissue<sup>20, 21, 22</sup>. Understanding the molecular mechanisms of SDH-related  
297 tumorigenesis provides a rationale for novel therapeutic interventions such as reversing the  
298 epigenetic abnormalities or exploiting metabolic vulnerabilities, similar to the recent  
299 discovery that tumoral 2-hydroxyglutarate accumulation may increase responsiveness to  
300 olaparib, a poly-ADP-ribose polymerase (PARP) inhibitor<sup>23</sup>. The availability of sensitive  
301 non-invasive biomarkers would greatly facilitate precision medicine-based clinical trials.  
302 Imaging with <sup>18</sup>F-FDG PET to measure the uptake and phosphorylation of a glucose-  
303 analogue to probe the increased glucose utilisation that occurs in many metabolically-active  
304 cancers, is a useful form of *in vivo* metabolic imaging and has been employed for the

305 detection of primary and metastatic disease in many tumour types including PPGL and  
306 GIST<sup>24, 25</sup> and is in widespread clinical use. However, despite being a very sensitive imaging  
307 tool, <sup>18</sup>F-FDG PET lacks specificity and cannot differentiate individual metabolites. <sup>1</sup>H-MRS  
308 is highly specific and allows *in vivo* detection of individual metabolites without the use of  
309 ionising radiation, however, <sup>1</sup>H-MRS is significantly less sensitive than PET, which could  
310 limit the detection of low levels of succinate and it can be challenging to differentiate  
311 intracellular from extracellular metabolites. In the future, <sup>1</sup>H-MRS may be complemented by  
312 other techniques such as hyperpolarised <sup>13</sup>C-MR spectroscopic imaging, which can increase  
313 MR signal-to-noise by several orders of magnitude allowing assessment of enzyme flux *in*  
314 *vivo*<sup>26</sup>.

315

316 We have shown that <sup>1</sup>H-MRS could be a valuable tool for the assessment of tumour response  
317 in the context of radionuclide and other therapies as alterations in succinate levels were  
318 detected despite stable appearances of the tumour diameter. This important application of <sup>1</sup>H-  
319 MRS could be expanded to include other tumours with specific metabolic defects including  
320 fumarate hydratase deficient tumours<sup>27</sup>, *IDH1* mutant tumours<sup>28</sup> and the recently identified  
321 malate dehydrogenase 2 (MDH2) deficient tumours<sup>29</sup>. However, important limitations of *in*  
322 *vivo* metabolomic analysis using <sup>1</sup>H-MRS were also revealed by our study: for example,  
323 spectral quality was poor in close proximity to metal dental work, adjacent to air spaces  
324 including the lung, in bone metastases, and was susceptible to motion artefact. In this study,  
325 the technical failure rate was 26%, which is similar to the failure rate reported in previous  
326 studies using <sup>1</sup>H-MRS<sup>16</sup>. Importantly, no cases was excluded from this prospective study,  
327 with the intention that this would inform on the translation of this imaging modality into  
328 clinical practice. Based on the evidence from this exploratory study, we would recommend  
329 that tumours were selected for <sup>1</sup>H-MRS analysis based on: (i) ideally the largest tumour

330 deposit but at least a size greater than 2 cm, (ii) tumours located close to bone or lung should  
331 be avoided, (iii) tumours with significant necrosis or hemorrhage should be avoided, (iv)  
332 superficial tumour deposits should be selected preferentially, and (v) respiratory triggered  
333 acquisition should be used for tumours in the upper abdomen, such as hepatic metastases.  
334 Although the use of <sup>1</sup>H-MRS as a diagnostic tool is likely to be limited to specialist centres,  
335 the number of scan averages in our study during spectral acquisition was less than half those  
336 reported in a previous study<sup>16</sup> (200 versus 512), without demonstrating a reduction in  
337 sensitivity. Using fewer scan averages reduces the acquisition time, making it more cost  
338 effective and convenient for the patient. This is a particularly important consideration if this  
339 imaging technique is to be considered for routine clinical practice or for sequential follow-up  
340 as part of a clinical trial. Furthermore this imaging modality could be used to investigate  
341 other metabolically-driven tumours.

342

343 In conclusion, this study is the largest to date to evaluate <sup>1</sup>H-MRS in patients with SDH  
344 deficiency. It has revealed that <sup>1</sup>H-MRS has the potential to be used as a non-invasive  
345 biomarker in the precision management of SDH-deficient disease and could have a role as a  
346 biomarker of successful treatment response. Lessons learned from this study could be applied  
347 to other similar metabolically-driven tumours.

348

349

350

351

352

353 **References**

- 354 1. Astuti D, Latif F, Dallol A, et al. Gene mutations in the succinate dehydrogenase subunit  
355 SDHB cause susceptibility to familial pheochromocytoma and to familial paraganglioma. *Am*  
356 *J Hum Genet* 2001;69:49–54.
- 357 2. Baysal BE, Ferrell RE, Willett-Brozick JE, et al. Mutations in SDHD, a mitochondrial  
358 complex II gene, in hereditary paraganglioma. *Science*. 2000 Feb 4;287(5454):848-51.
- 359 3. K.A. Janeway, S.Y. Kim, M. Lodish, et al. Defects in succinate dehydrogenase in  
360 gastrointestinal stromal tumors lacking KIT and PDGFRA mutations. *Proc. Natl. Acad. Sci.*  
361 *USA* 2011;108, 314–318.
- 362 4. Vanharanta S, Buchta M, McWhinney SR, et al. Early-onset renal cell carcinoma as a  
363 novel extraparaganglial component of SDHB-associated heritable paraganglioma. *Am J Hum*  
364 *Genet* 2004;74:153–159.
- 365 5. Xekouki P, Stratakis CA. Succinate dehydrogenase (SDHx) mutations in pituitary tumors:  
366 could this be a new role for mitochondrial complex II and/or Krebs cycle defects? *Endocr*  
367 *Relat Cancer* 2012;19:C33–C40.
- 368 6. Cecchini, G. Respiratory complex II: Role in cellular physiology and disease. *Biochim.*  
369 *Biophys. Acta (BBA)-Bioenerg.* 1827, 541–542 (2013).
- 370 7. Morin A, Letouzé E, Gimenez-Roqueplo AP, et al. Oncometabolites-driven tumorigenesis:  
371 From genetics to targeted therapy. *Int J Cancer*. 2014 Nov 15;135(10):2237-48. doi:  
372 10.1002/ijc.29080.
- 373 8. Pritchett JW. Familial occurrence of carotid body tumor and pheochromocytoma. *Cancer*  
374 1982 49 2578–2579.



- 375 9. Gimenez-Roqueplo AP, Favier J, Rustin P, et al. COMETE Network. Mutations in the  
376 SDHB gene are associated with extra-adrenal and/or malignant pheochromocytomas. *Cancer*  
377 *Res.* 2003;63:5615–5621.
- 378 10. Evenepoel L, Papathomas TG, Krol N, et al. Toward an improved definition of the  
379 genetic and tumor spectrum associated with SDH germ-line mutations. *Genet Med.* 2015  
380 Aug;17(8):610-20. doi: 10.1038/gim.2014.162.
- 381 11. Boikos SA, Pappo AS, Killian JK, et al. Molecular Subtypes of KIT/PDGFR Wild-  
382 Type Gastrointestinal Stromal Tumors: A Report from the National Institutes of Health  
383 Gastrointestinal Stromal Tumor Clinic. *JAMA Oncol.* 2016 Jul 1;2(7):922-8. doi:  
384 10.1001/jamaoncol.2016.0256.
- 385 12. Mason EF, Hornick JL. Conventional Risk Stratification Fails to Predict Progression of  
386 Succinate Dehydrogenase-deficient Gastrointestinal Stromal Tumors: A Clinicopathologic  
387 Study of 76 Cases. *Am J Surg Pathol.* 2016 Jun 23.
- 388 13. Ricketts C, Woodward ER, Killick P, et al. Germline SDHB mutations and familial renal  
389 cell carcinoma. *J Natl Cancer Inst.* 2008 Sep 3;100(17):1260-2. doi: 10.1093/jnci/djn254.
- 390 14. Amar L, Fassnacht M, Gimenez-Roqueplo AP, et al. Long-term postoperative follow-up  
391 in patients with apparently benign pheochromocytoma and paraganglioma. *Hormone and*  
392 *Metabolic Research* 2012 44 385–389.
- 393 15. Richter S, Peitzsch M, Rapizzi E, et al. Krebs cycle metabolite profiling for identification  
394 and stratification of pheochromocytomas/paragangliomas due to succinate dehydrogenase  
395 deficiency. *J Clin Endocrinol Metab* 2014;99:3903–11.

- 396 16. Varoquaux A, le Fur Y, Imperiale A, et al. Magnetic resonance spectroscopy of  
397 paragangliomas: new insights into in vivo metabolomics. *Endocr Relat Cancer*. 2015  
398 Aug;22(4):M1-8. doi: 10.1530/ERC-15-0246. Epub 2015 Jun 26.
- 399 17. Lussey-Lepoutre C, Bellucci A, Morin A, et al. In Vivo Detection of Succinate by  
400 Magnetic Resonance Spectroscopy as a Hallmark of SDHx Mutations in Paraganglioma. *Clin*  
401 *Cancer Res*. 2016 Mar 1;22(5):1120-9. doi: 10.1158/1078-0432.CCR-15-1576. Epub 2015  
402 Oct 21.
- 403 18. Andronesi OC, Rapalino O, Gerstner E, et al. Detection of oncogenic IDH1 mutations  
404 using magnetic resonance spectroscopy of 2-hydroxyglutarate. *J Clin Invest*. 2013  
405 Sep;123(9):3659-63. doi: 10.1172/JCI67229.
- 406 19. Provencher SW. Estimation of metabolite concentrations from localized in vivo proton  
407 NMR spectra. *Magn Reson Med*. 1993 Dec;30(6):672-9.
- 408 20. Xu, W, Yang, H., Liu, Y., et al. (2011). Oncometabolite 2-hydroxyglutarate is a  
409 competitive inhibitor of  $\alpha$ -ketoglutarate-dependent dioxygenases. *Cancer Cell* 19,17–30.
- 410 21 Letouze, E , Martinelli C, Lorient C, et al. SDH mutations establish a hypermethylator  
411 phenotype in paraganglioma. *Cancer Cell* 23, 739–752 (2013).
- 412 22. Garrigue P, Bodin-Hullin A, Balasse L, et al. The evolving role of succinate in tumor  
413 metabolism: an  $^{18}\text{F}$ -FDG-based study. *J Nucl Med*. 2017 Jun 15. pii: jnumed.117.192674.  
414 doi: 10.2967/jnumed.117.192674.
- 415 23. Sulkowski PL, Corso CD, Robinson ND, et al. 2-Hydroxyglutarate produced by  
416 neomorphic IDH mutations suppresses homologous recombination and induces PARP  
417 inhibitor sensitivity. *Sci Transl Med*. 2017 Feb 1;9(375). pii: eaal2463. doi:  
418 10.1126/scitranslmed.aal2463.

- 419 24. Chang CA, Pattison DA, Tothill RW, et al.  $^{68}\text{Ga}$ -DOTATATE and  $^{18}\text{F}$ -FDG PET/CT in  
420 Paraganglioma and Pheochromocytoma: utility, patterns and heterogeneity. *Cancer Imaging*.  
421 2016 Aug 17;16(1):22. doi: 10.1186/s40644-016-0084-2.
- 422 25. Holdsworth CH, Badawi RD, Manola JB, et al. CT and PET: early prognostic indicators  
423 of response to imatinib mesylate in patients with gastrointestinal stromal tumor. *AJR Am J*  
424 *Roentgenol* 2007;189:W324-30.
- 425 26. Day SE, Kettunen MI, Gallagher FA, et al. Detecting tumor response to treatment using  
426 hyperpolarized  $^{13}\text{C}$  magnetic resonance imaging and spectroscopy. *Nat Med*. 2007  
427 Nov;13(11):1382-7. Epub 2007 Oct 28. Erratum in: *Nat Med*. 2007 Dec;13(12):1521.
- 428 27. Clark GR, Sciacovelli M, Gaude E, et al. Germline FH mutations presenting with  
429 pheochromocytoma. *J Clin Endocrinol Metab*. 2014 Oct;99(10):E2046-50.
- 430 28. Andronesi OC, Rapalino O, Gerstner E, et al. Detection of oncogenic IDH1 mutations  
431 using magnetic resonance spectroscopy of 2-hydroxyglutarate. *J Clin Invest*. 2013  
432 Sep;123(9):3659-63. doi: 10.1172/JCI67229.
- 433 29. Cascón A, Comino-Méndez I, Currás-Freixes M, et al. Whole-exome sequencing  
434 identifies MDH2 as a new familial paraganglioma gene. *J Natl Cancer Inst*. 2015 Mar  
435 11;107(5). pii: djv053. doi: 10.1093/jnci/djv053.
- 436 30. Madhu B, Shaw GL, Warren AY, et al. Response of Degarelix treatment in human  
437 prostate cancer monitored by HR-MAS  $^1\text{H}$  NMR spectroscopy. *Metabolomics*. 2016;12:120
- 438 31. Andreasson A, Kiss NB, Caramuta S, et al. The VHL gene is epigenetically inactivated in  
439 pheochromocytomas and abdominal paragangliomas. *Epigenetics*. 2013 Dec;8(12):1347-54.  
440 doi: 10.4161/epi.26686. Epub 2013 Oct 22.

441

442 **Funding:**

443 **We thank the following funding organisations; GIST Support UK (RC), Cambridge**  
444 **Experimental Cancer Medicine Centre, Addenbrooke’s Charitable Trust, National**  
445 **Institute for Health Research (NIHR) Cambridge Biomedical Research Centre, Cancer**  
446 **Research UK CRUK (FAG, MM), CRUK Cambridge Centre (MM, FAG, ERM), the**  
447 **University of Cambridge, and Hutchison Whampoa Ltd (MM), NIHR Senior**  
448 **Investigator Award (ERM), European Research Council Advanced Researcher Award**  
449 **(ERM), the British Heart Foundation (ERM), CRUK and Engineering and Physical**  
450 **Sciences Research Council (EPSRC) Imaging Centre in Cambridge and Manchester**  
451 **(FAG). The University of Cambridge has received salary support in respect of EM from**  
452 **the NHS in the East of England through the Clinical Academic Reserve.**

453

454 **Acknowledgements:**

455 **The authors would like to thank Stephen Provencher for providing the simulated basis**  
456 **set used in spectral fitting, the radiographers and staff of the MRIS Unit at**  
457 **Addenbrooke’s Hospital and the staff of the Tissue Bank at Addenbrooke’s hospital for**  
458 **assistance, and all the patients who participated in this study.**

459

460

461

462

463

464 **Tables:**

465 **Table 1:** Clinical characteristics of the cohort. PA = pituitary adenoma, PC =

466 pheochromocytoma.

Case number	Genetic mutation	Sex	Age	Primary tumour	Metastatic disease	Site of metastatic disease	Family history	Other primary tumour
1	<i>SDHC</i> epimutation	F	21	GIST	Yes	Liver, lung	No	No
2	<i>SDHB</i> c.268C>T p.(Arg90* )	F	53	Abdominal PGL	Yes	Lymph nodes, bone	Yes- mother (GIST)	No
3	<i>SDHC</i> epimutation	F	25	GIST	Yes	Liver	No	No
4	No mutation detected	F	27	GIST	No	NA	No	No
5	<i>SDHB</i> c.137G>A p.(Arg46Gln)	M	38	GIST	Yes	Liver, peritoneum	No	No
6	<i>SDHB</i> c.380G>T p.(Ile127Ser)	M	80	PA	No	NA	Yes nephew (PPGL)	No
7	No mutation detected	M	70	PC	Yes	Liver, bone	No	No

8	<i>SDHB</i> c.600G>T p.(Trp200Cys)	M	41	Glomus PGL	No	NA	No	Yes, PA
9.	<i>SDHB</i> c.302G>A p.(Cys101Tyr)	M	26	Abdomin al PGL	No	NA	No	Carotid PGL
10.	No mutation detected	M	23	PC	No	NA	No	No
11.	<i>SDHA</i> c.91C>T p.(Arg31Ter)	F	21	GIST	Yes	Liver	No	No
12.	<i>SDHA</i> c.1765C>T p.(Arg589Trp)	F	37	GIST	Yes	Liver	No	No
13	<i>SDHA</i> c.91C>T p.(Arg31Ter)	M	46	PGL	Yes	Bone	No	No
14	<i>SDHA</i> c.91C>T p.(Arg31Ter)	M	24	GIST	Yes	Liver	No	No
15	No mutation	M	67	PC	No	NA	No	No

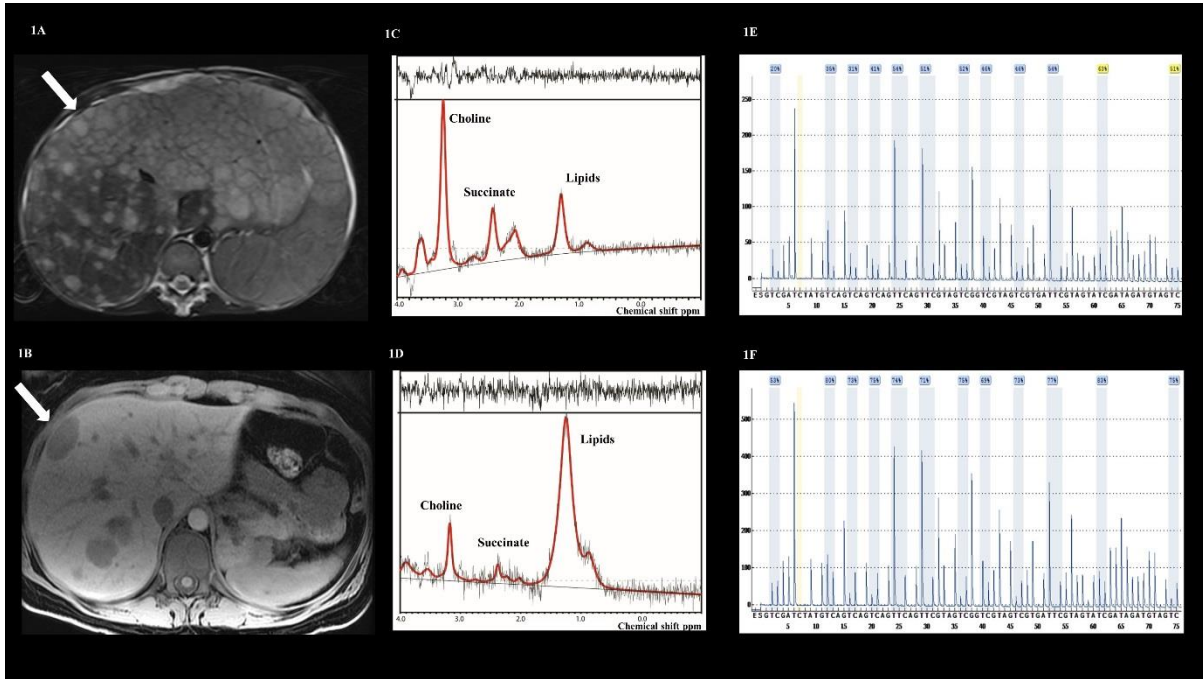
467

468 **Figure legends**

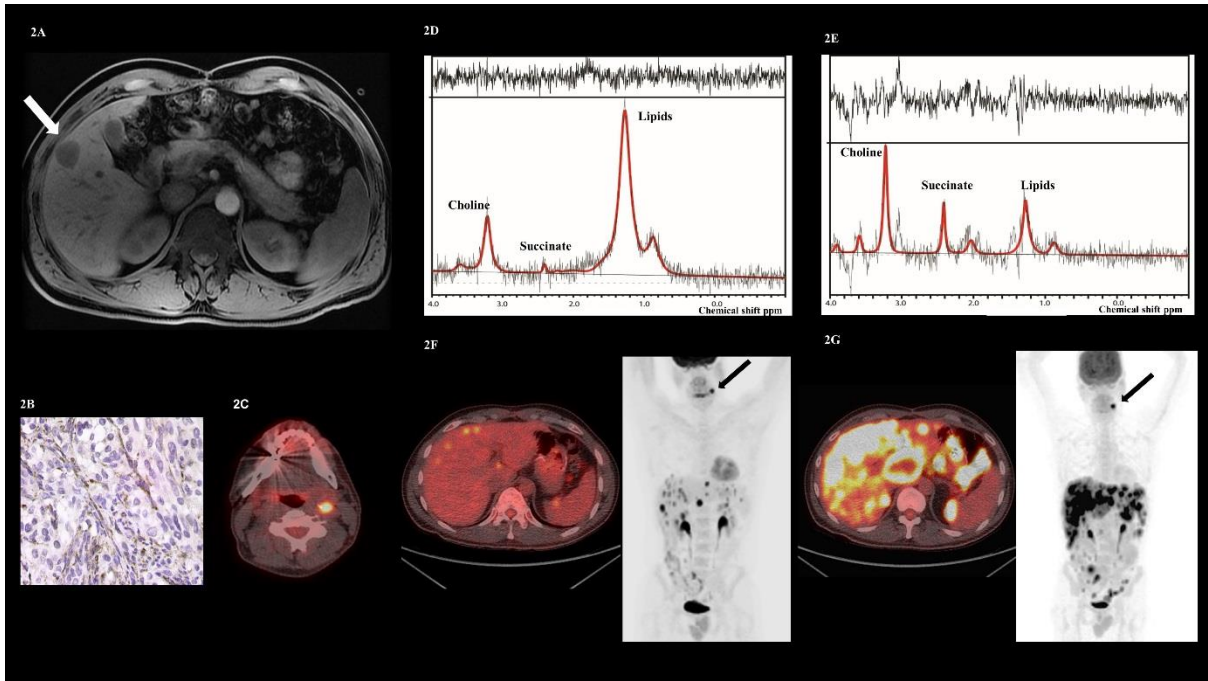
469 Figure 1. (A): T<sub>2</sub>-weighted MR image from case 1 and (B) T<sub>1</sub>-weighted image from case 3

470 demonstrating liver metastases from which spectra were acquired in the locations indicated

471 by the white arrows. (C-D) show the spectra from case 1 and case 3 demonstrating a  
 472 succinate peak at 2.4 ppm. (E-F) demonstrate hypermethylation of the promoter region of the  
 473 SDHC gene in tumour DNA from cases 1 and 3, confirming a somatic SDHC epimutation:  
 474 55% mean methylation in case 1 and 75% mean methylation in case 3.



475  
 476  
 477 Figure 2. (A) T<sub>1</sub>-weighted MR image of a metastatic GIST to the liver (arrow) from case 5.  
 478 (B) SDHB immunonegativity on SDHB immunohistochemistry performed on the wt GIST  
 479 tumour from the same patient. (C) Axial fused <sup>18</sup>F-FDG PET/CT image demonstrating an  
 480 FDG-avid carotid body PGL after SDH deficiency was demonstrated on <sup>1</sup>H-MRS. (D-E)  
 481 Spectra acquired at <sup>1</sup>H-MRS from the same case before and during treatment with a multi-  
 482 kinase inhibitor. (F-G) Axial fused <sup>18</sup>F-FDG PET/CT images and corresponding coronal PET  
 483 projections illustrating the increase in disease burden and FDG avidity over time (SUV: 15.1  
 484 and 27.1) which correlates with the increase in the succinate peak demonstrated on <sup>1</sup>H-MRS.

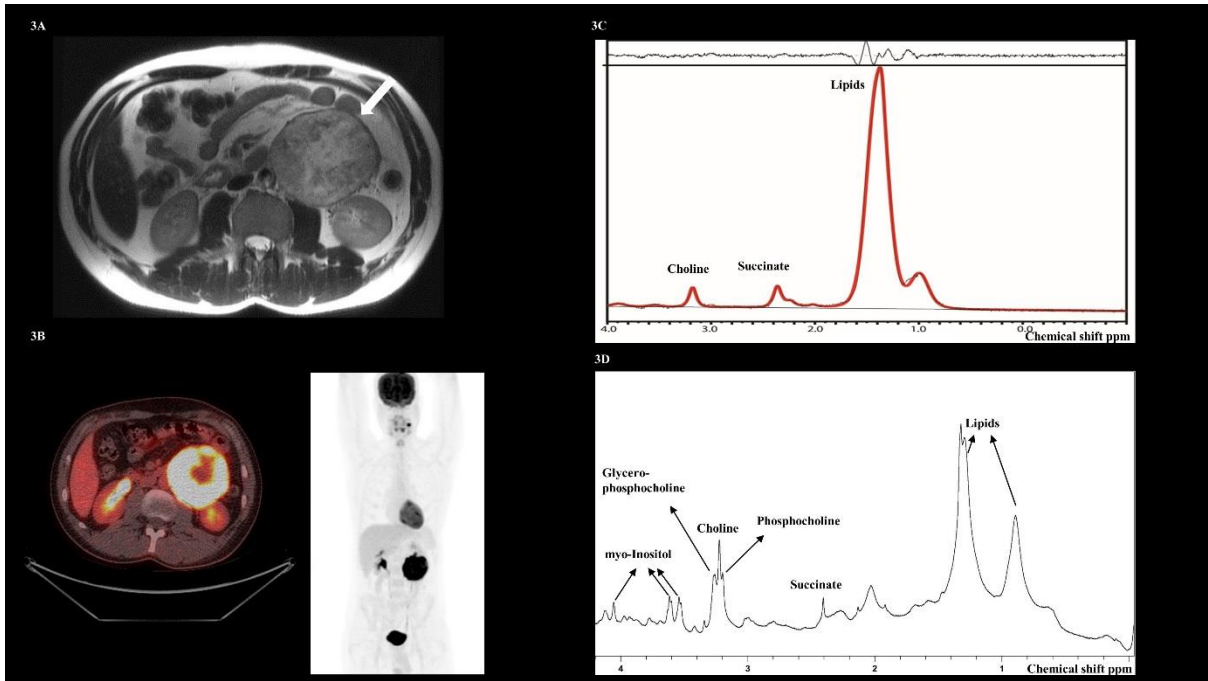


485

486

487 Figure 3. (A) T<sub>2</sub>-weighted MRI showing a large non-secretory abdominal paraganglioma  
 488 from case 9 (arrow). (B) <sup>1</sup>H-MR spectra demonstrating a succinate peak at 2.4 ppm. (C) Axial  
 489 fused <sup>18</sup>F-FDG PET/CT image. The corresponding coronal maximum intensity projection  
 490 (MIP) PET image demonstrates a synchronous left sided carotid paraganglioma. (D) Spectra  
 491 acquired by High Resolution Magic Angle Spinning (HR-MAS) *in vitro* on the  
 492 paraganglioma tumour sample, again confirming a succinate peak at 2.4 ppm.

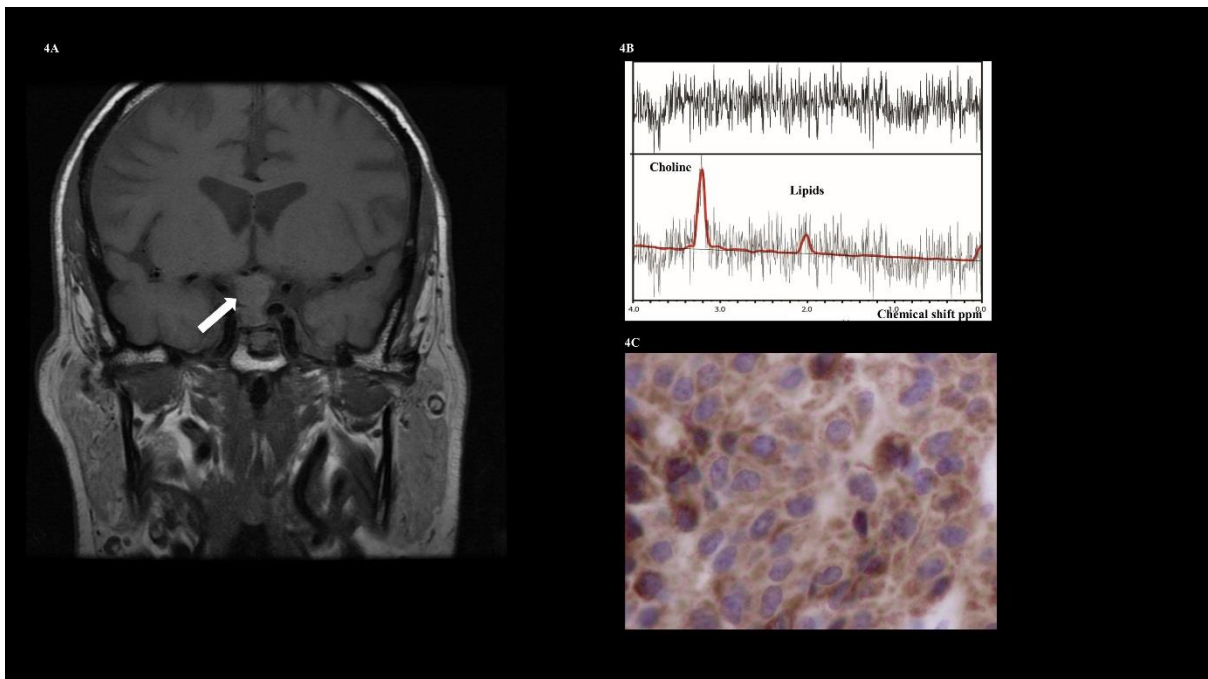




493

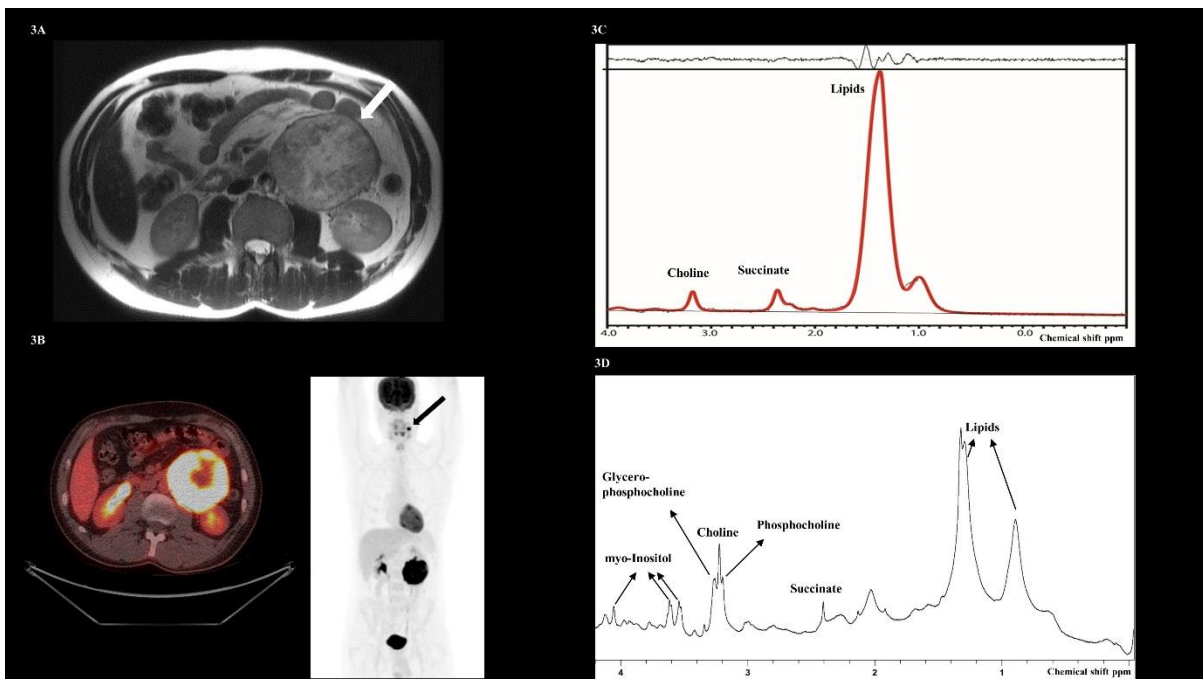
494

495 **Figure 4:** (A) Coronal T<sub>1</sub>-weighted MRI demonstrating a remnant pituitary adenoma in case  
 496 6 (white arrow). (B) Spectra acquired from the pituitary tumour at <sup>1</sup>H-MRS, with evidence of  
 497 choline detection but no succinate. (C) SDHB IHC demonstrating preservation of the SDHB  
 498 protein performed on a section of tumour tissue debulked from the pituitary tumour.



499

500 Figure 5. (A) Axial T<sub>2</sub>-weighted MRI image of a retroperitoneal nodal metastases from case 2  
501 (arrow). (B) Spectra acquired before treatment illustrating succinate accumulation at 2.4 ppm.  
502 (C) Spectra acquired following 4 cycles of [<sup>177</sup>Lu]-DOTATATE with no detectable succinate  
503 peak at 2.4 ppm. (D) Plasma metanephrine and methoxytyramine levels before and after  
504 treatment with [<sup>177</sup>Lu]-DOTATATE. (E) Axial fused <sup>18</sup>F-FDG PET/CT image and  
505 corresponding coronal PET projection showing the FDG-avid nodal metastases (SUV = 16.1,  
506 arrowed). (F) The same nodal metastases following treatment with [<sup>177</sup>Lu]-DOTATATE  
507 demonstrating reduced tracer uptake in keeping with the biochemical findings (SUV = 9.3).



508

509

510

511

512

513

514

515 **Supplementary data:**

516 Figure S1: (A) Coronal MRI image of a large left sided glomus paraganglioma from case 8  
517 demonstrated by the white arrow. (B) Spectra processed with LCModel from the same patient  
518 showing a broad unreliable peak at 2.4 ppm, which was not convincing for succinate.

519 Table S1: Characteristics of the 15 tumours analysed by <sup>1</sup>H-MRS. TF: technical failure,  
520 defined as an estimated uncertainty (%SD) > 15% in automated peak fitting of choline using  
521 LCModel. ND: not detected. NA: not applicable.

522 Table S2: Characteristics of the two patients in whom <sup>1</sup>H-MRS was repeated during the same  
523 examination to evaluate test reproducibility.

524